sciendo
ISSN 1335-8871
MEASUREMENT SCIENCE REVIEW
Journal homepage: https://content.sciendo.com

Glucose Concentration Monitoring Using Microstrip Spurline Sensor

Supakorn Harnsoongnoen[1*], Benjaporn Buranrat[2]

[1]*The Biomimicry for Sustainable Agriculture, Health, Environment and Energy Research Unit, Department of Physics, Faculty of Science, Mahasarakham University, Kantarawichai District, Maha Sarakham, 44150, Thailand, supakorn.h@msu.ac.th*
[2]*Faculty of Medicine, Mahasarakham University, Muang District, Maha Sarakham 44000, Thailand, buranrat.b@msu.ac.th*

Abstract: This article reports a microstrip spurline sensor for glucose concentration monitoring. The microstrip spurline sensor is a low-cost and easy-to-fabricate device that uses printed circuit board (PCB) technology. It consists of a combination of four spurlines and transmission lines. The four spurlines are used to reject unwanted frequencies, while the transmission lines allow the desired frequencies to pass through. The resonance frequency (F_r) and reflection coefficient (S_{11}) were recorded through meticulous simulations and experiments over a frequency range from 1.5 GHz to 4 GHz. In addition, the sensor was used to detect changes in glucose concentration, ranging from 0 mg/dL to 150 mg/dL. The findings of this study show that the antenna-based sensor proposed in this research can effectively measure glucose levels across the diabetes range, from hypoglycemia to normoglycemia to hyperglycemia, with a high degree of sensitivity of 7.82 x 10^{-3} dB/(mg/dL) and 233.33 kHz/(mg/dL).

Keywords: Microwave sensor, glucose sensing, microstrip spurline, noninvasive, microwave frequencies, diabetes

1. INTRODUCTION

Diabetes, a chronic metabolic disorder affecting millions of people worldwide [1], makes the measurement of glucose concentration essential for accurate diagnosis and effective management [2]. Traditional methods of glucose measurement, such as blood glucose meters, are invasive and require frequent blood sampling, which can be inconvenient and painful [3]. A plethora of noninvasive glucose measurement techniques exist, including near-infrared (NIR) spectroscopy [4], mid-infrared (MIR) spectroscopy [5], photoacoustic (PA) spectroscopy [6], Raman spectroscopy [7], fluorescence spectroscopy [8], optical coherence tomography (OCT) [9], terahertz (THz) spectroscopy [10], and microwave sensing, all of which have been extensively researched. Microwave sensors offer a non-invasive alternative for glucose measurement, which has gained significant attention in recent years [11]. Microwave sensors use the interaction between microwave radiation and the sample to measure the physical properties of the sample [12]. Due to the lower energy per photon and less atmospheric scattering, microwave radiation can penetrate deeper into the tissue, enabling more accurate measurement of blood glucose data [13]. The design of microwave sensors is intricately linked to the dielectric properties of tissues, as reflected, transmitted, and absorbed microwaves interact closely with them. These properties are affected by glucose fluctuations, as the relative permittivity varies accordingly [14], [15]. Glucose molecules have high relative permittivity, which makes them an ideal candidate for microwave-based sensing [16]. Several techniques have been developed for measuring glucose concentration using microwave sensors that measure the complex permittivity of the sample [17]-[25]. Nevertheless, the identification of the precise correlation between glucose levels and effective permittivity remains a critical challenge for microwave sensors. Ongoing research endeavors are focused on improving the selectivity [26]-[28] and sensitivity [29], [30] of microwave sensors. Regarding selectivity, the dielectric properties of tissues represent an average value, and their fluctuations could be attributed to a variety of tissue components. Therefore, further studies may be required to determine how the changes in dielectric properties correspond to blood glucose levels [31]-[38]. In this paper, a compact microwave sensor for monitoring glucose concentration is proposed. The sensor uses four spurlines of appropriate length inserted into a patch antenna, which enables effective rejection bandwidth and deeper rejection of the proposed filter. The proposed design is described in detail, and simulations and experiments are performed. Finally, the simulated and experimental results are presented and discussed.

DOI: 10.2478/msr-2023-0022
**Corresponding author: supakorn.h@msu.ac.th (S. Harnsoongnoen)*

2. MATERIALS AND METHODS

A. Design and fabrication of the sensor

The architecture of the sensor consists of two double spurline filters, shown in Fig. 1(a). Fig. 1(b) shows both the top and bottom views of the proposed sensor fabrication process. The proposed sensor was fabricated using the photolithography technique, which is a simple process.

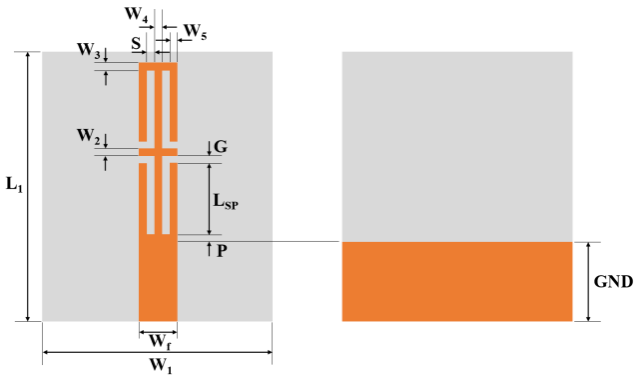

(a)

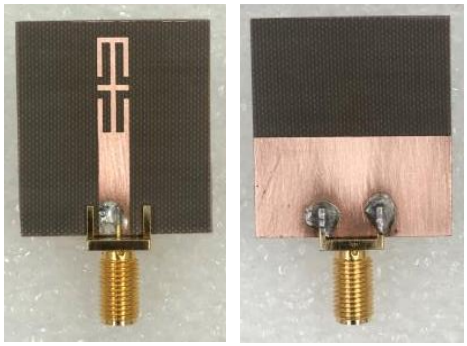

(b)

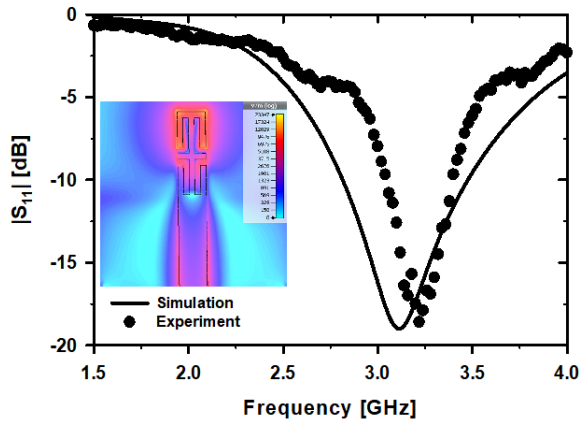

(c)

Fig. 1. The proposed microwave sensor, (a) schematic and (b) fabricated sensors and (c) S_{11} spectra and electric field distribution, the geometrical parameters of a proposed sensor were W_1 = 35 mm, W_f = 5 mm, L_1 = 32 mm, GND = 15 mm, P = 1 mm, L_{SP} = 5 mm, G = 1 mm, W_2 = 1 mm, W_3 = 1 mm, W_4 = 1 mm, W_5 = 1 mm, S = 1 mm.

A DiClad880 substrate with thickness of 1.6 mm, a double-sided copper thickness of 35 μm, a relative permittivity (ε_r) of 2.2, and a loss tangent of 0.0009 was used to fabricate the sensor device. The sensor was fabricated on a printed circuit board (PCB) using a negative dry film photoresist technique. Fig. 1(c) shows the spectra of the reflection coefficients, ranging from 1.5 GHz to 4 GHz, for both the simulated and experimental results. The simulated reflection coefficient was determined to be -18.99 dB, while the experimental reflection coefficient was -18.60 dB, indicating a difference of 2.07%. The simulated resonance frequency (F_r) was determined to be 3.12 GHz, while the experimental F_r was measured at 3.22 GHz, resulting in a difference of 3.11%. The electric field distribution at a 0 degree phase angle of the proposed sensor is shown in the inset image in Fig. 1(c) by full-wave electromagnetic simulation. The analysis revealed that the strength of the electric field was concentrated from the two double spurlines to the top end of the sensor.

B. Sample under test area

Fig. 2 shows a simulation depicting the effect of sample area ($W_{SUT} \times L_{SUT}$) on the reflection coefficient (S_{11}) spectra of spurline microstrip sensors, where W_{SUT} is the width of the sample under test (SUT), which is an aqueous solution, and L_{SUT} is the length of the SUT. The W_{SUT} is fixed (6 mm), while the L_{SUT} can be set to various values. The L_{SUT} ranges in size from 0.5 to 15.5 in steps of 1.0 mm.

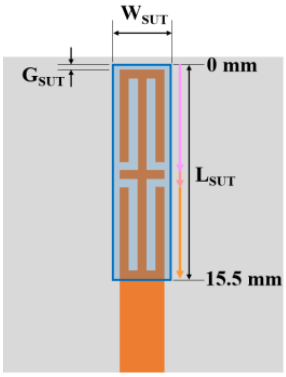

(a)

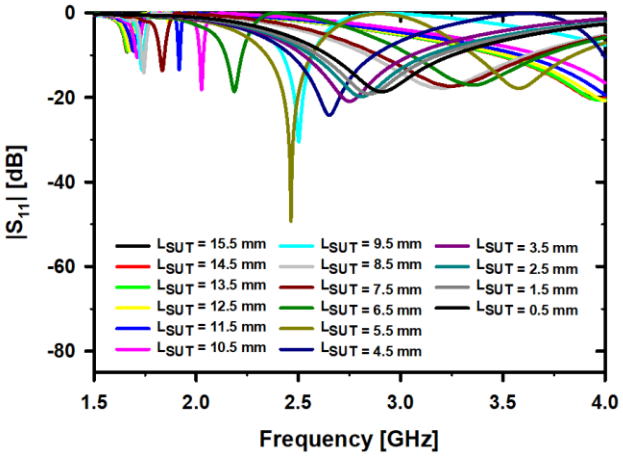

(b)

Fig. 2. The simulation involves analyzing S_{11} spectra with varying area of the SUT (a) the sensor's structure with varying L_{SUT} and (b) S_{11} spectra with varying L_{SUT} from 0.5 to 15.5 mm with an increase step of 1.0 mm, where L_{SUT} is the length of the SUT, G_{SUT} = 0.5 mm, and W_{SUT} = 6 mm.

Fig. 2(a) shows the structure of the sensor and the location where the aqueous test medium (permittivity (ε_r) = 78.4) was introduced. On the other hand, Fig. 2(b) shows the S_{11} spectra of the test regions covering lengths from 0.5 to 15.5 mm. We found that for a frequency range from 1.5 GHz to 4 GHz, the L_{SUT} located 5.5 mm and 9.5 mm from the top of the sensor resulted in the tallest $|S_{11}|$ compared to other lengths. This observation could be attributed to the fact that the region between 5.5 mm and 9.5 mm is the most sensitive and responsive to the sample being tested. Based on this observation, we chose the L_{SUT} position between 5.5 mm and 9.5 mm as the chamber location for measuring the sample in this study.

C. *Chemicals and analyte solution preparation*

To prepare a series of water-glucose solutions with different concentrations, we mixed D-glucose powder from Sigma-Aldrich (USA) with distilled water. We prepared four sets of glucose solutions, with concentrations of 35.7, 50, 75, and 150 mg/dL, respectively. The normal range for blood glucose concentration in the body is between 70 and 120 mg/dL, but this value may vary slightly depending on the time of day and the laboratory performing the test. In addition, glucose concentration may fluctuate due to various factors such as the time of day and the presence of medical conditions such as diabetes. To ensure that our experiment covered the levels present in normal, latent, and diabetic subjects, we selected a glucose concentration range. Each concentration was prepared in triplicate.

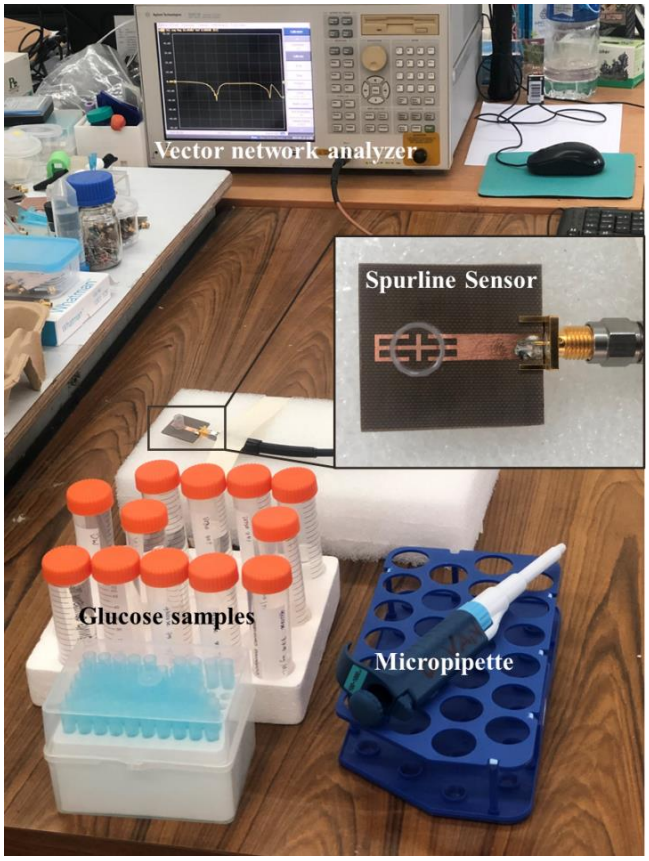

Fig. 3. Measurement setup.

D. *Experimental measurement setup*

Fig. 3 shows the setup of the sensor and the measuring device. The sensor is mounted on a foam base and connected to a Vector Network Analyzer (VNA) using a high-frequency cable. The S_{11} value is measured and recorded after calibrating Port 1 of the VNA using the short-open-load (SOL) calibration procedure. The measurements were performed on samples with a volume of 50 µL at room temperature, starting with low glucose concentrations and gradually increasing to higher levels. The test solution is filled into the chamber tube using a micro-pipette. The chamber tube is rinsed and cleaned with DI water after each measurement to ensure reliability and consistency. Three measurements are taken for each glucose solution sample at each concentration to ensure accuracy. The frequency range of 1.5 - 4 GHz is used for each measurement. To obtain this data, various sample tests are performed, including free space, an empty tube, DI water, and various glucose concentrations.

3. RESULTS AND DISCUSSION

A. *Reflection coefficient of sensor sensing*

After selecting the location for the sample chamber in the test, we ran simulations to evaluate the response of the sensors to changes in relative permittivity. The structure of the sensor with a cylindrical chamber and a diameter of 8 mm is shown on the left in Fig. 4(a). The actual sensor structure, which includes a cylindrical chamber with a height (H_C) of 6 mm, is shown on the right. Fig. 4(b) shows the S_{11} spectra obtained in the simulation. These spectra were generated by varying the relative permittivity of the samples at 20, 40, 60, and 80, while maintaining a constant volume for all simulation variants (the radius is 4 mm and the thickness is 1 mm). The simulation results show that changes in the relative permittivity values lead to changes in both the S_{11} magnitude and resonant frequency F_r. Equation (1) represents the nonlinear relationship between the relative permittivity and $|S_{11}|$, as obtained from the simulation results shown in Fig. 4(c). F_r also exhibits a nonlinear relationship with the relative permittivity, as shown in (2). The coefficient of determination (R^2) of both trend equations is equal to 1. It was found that an increase in relative permittivity leads to an increase in $|S_{11}|$ and a decrease in resonant frequency.

$$|S_{11}| = -68.98 + 61.36(1 - e^{-0.0587\varepsilon_r}) \quad (1)$$

$$F_r = 1.24 + 1.81e^{-0.0184\varepsilon_r} \quad (2)$$

The changes in $|S_{11}|$ vary with the increase in relative permittivity (ε_r) and can be attributed to the corresponding changes in the total resistance of the sensor. The change in F_r is a result of the corresponding change in relative permittivity. The change in both is influenced by the glucose concentration [31]. The reported measurement results confirm that as glucose levels increase, relative permittivity of the mixture decreases at lower frequencies [16], [32], [33]. However, it should be noted that the range of glucose concentration studied in this research was limited to 0 mg/dL to 150 mg/dL, which may have affected the changes in total resistivity and relative permittivity within the narrow measurement region. Other factors that may have influenced these changes are discussed in the next section.

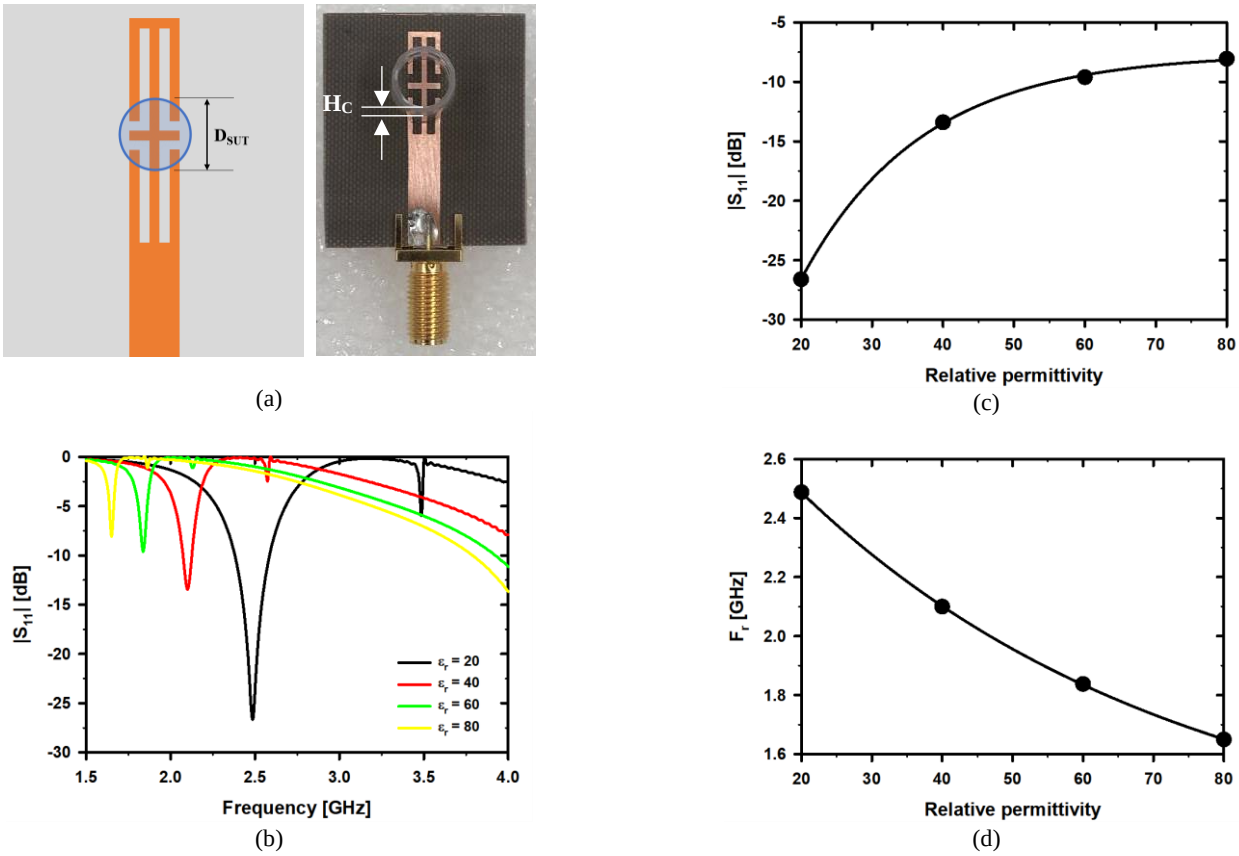

Fig. 4. Position and active area for sample under test sensing, (a) sensor layout and fabricated sensor with cylindrical chamber tube setup, D_{SUT} is the diameter of chamber for SUT, D_{SUT} = 8 mm, (b) simulated S-parameters of a microstrip spurline sensor with varying relative permittivity (ε_r), (c) relationship between ε_r and $|S_{11}|$, and (d) relationship between ε_r and F_r.

B. Amplitude and frequency variation

The S_{11} spectra obtained from measurements of different glucose concentrations are shown in Fig. 5. When observing $|S_{11}|$ and the Fr with increasing glucose concentrations, it was found that both values changed as the glucose concentration varied, as shown in the enlarged figure. Fig. 6(a) shows the relationship between $|S_{11}|$ and glucose concentration in the range from 0 mg/dL to 150 mg/dL, which can be divided into two concentration ranges: the range from 0 mg/dL to 50 mg/dL and the range from 50 mg/dL to 150 mg/dL. In the concentration range from 0 mg/dL to 50 mg/dL, a non-linear relationship was observed between $|S_{11}|$ and glucose concentration (black solid line), as shown in (3). In the range from 50 mg/dL to 150 mg/dL, a non-linear relationship between $|S_{11}|$ and glucose concentration was also observed (blue solid line), as shown in (4).

The existence of two distinct trends in $|S_{11}|$ regarding concentration in the range from 0 mg/dL to 150 mg/dL in this study is incongruent with the monotonic curves typically observed in the vast majority of previously published works [38]-[41]. This deviation in behavior may be attributed to electronic noise and environmental factors, or possibly to sample instability at concentrations of 37.5 and 50.0 mg/dL, which may have significantly affected the measurements at these levels as opposed to higher concentrations [38]. Therefore, a definitive conclusion regarding the exact cause cannot be drawn with absolute certainty.

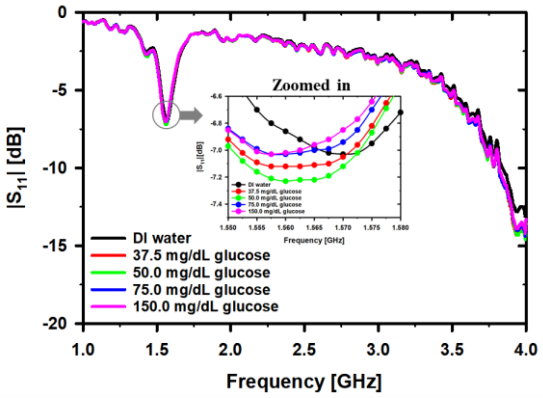

Fig. 5. The S_{11} spectra for various SUTs.

$$|S_{11}| = -7.0347 + 0.0015\rho - 0.0001\rho^2 \quad (3)$$

$$|S_{11}| = -\frac{1.775\rho}{(-18.94+\rho)} - \frac{5.37\rho}{(11.44+\rho)} \quad (4)$$

However, when the relationship between F_r and glucose concentration (in mg/dL units) was examined, a uniformly non-linear relationship was observed across the concentration range from 0 mg/dL to 150 mg/dL, as shown in (5), which has an R^2 value of 0.9739.

$$F_r = 1.56 \times 10^9 + 11.61 \times 10^6 e^{(-0.0427\rho)} \quad (5)$$

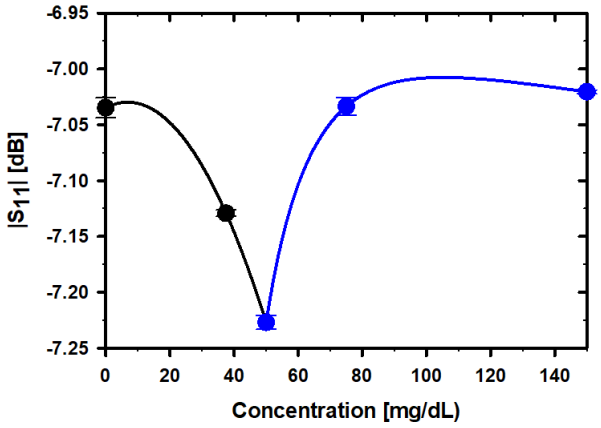

(a)

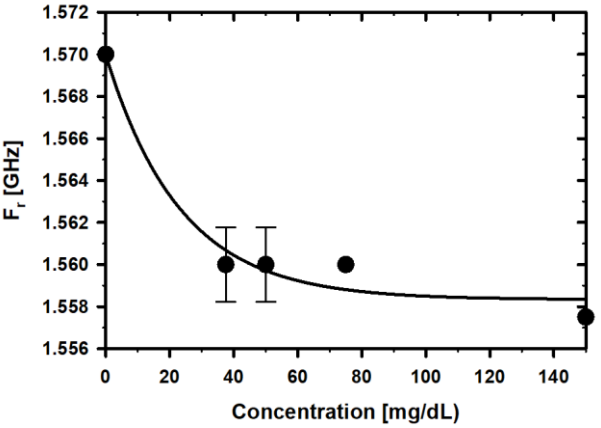

(b)

Fig. 6. The magnitude of S_{11} and F_r for various glucose concentrations, (a) $|S_{11}|$ and (b) F_r for different glucose concentrations in the concentration range from 0 mg/dL to 150 mg/dL.

Based on glucose measurements ranging from 0 mg/dL to 150 mg/dL, $|S_{11}|$ values had the highest and lowest values of -7.02 dB and -7.23 dB, respectively, corresponding to a difference of -0.21 dB. In addition, the highest and lowest resonance frequencies of 1.570 GHz and 1.558 GHz, respectively, were observed, corresponding to a difference of 12.50 MHz. After measuring glucose concentration with the proposed sensor, our results show that a gradual decrease of $|S_{11}|$ occurs as a quadratic polynomial within the concentration range from 0 to 50 mg/dL. This may be attributed to the increased resistivity of substances when glucose is present in this range. Nevertheless, when the glucose concentration was increased from 50 mg/dL to 150 mg/dL, an increase in the $|S_{11}|$ value was observed. This may be attributed to higher electrical conductivity of the total test substance within this concentration range [32], [36], [37]. When examining the relationship between F_r and glucose concentration within the study range, it was found that the measured F_r of the proposed sensor increased with higher glucose concentrations [38].

C. Comparison of the performance of the proposed sensor

Table 1 shows a performance comparison of sensors from the literature and the sensor proposed in this work. The detection pattern of the sensor exhibits both amplitude and frequency variations. The sensitivity of the two parameters of each sensor was calculated and is shown in the table. Compared to other structural sensors, the sensor presented in this paper has an outstanding feature of operating at low frequencies with a small volume sample and has high sensitivity in both magnitude and frequency variation measurements.

Table 1. An analysis of diverse methods in detecting glucose levels utilizing microwave sensors.

Ref.	**Technique**	**Concentration (mg/dL)**	**Sensing parameters**	**F_r (GHz)**	**Volume (µL)**	**Sensitivity**
30	Microstrip Patch Antenna-Sensor	0-400	F_r (S_{11})	2.4	NA	25 kHz/(mg/dL)
32	Open-ended coaxial probe	0-16.000	F_r (S_{11})	0.3-15	NA	NA
33	Hilbert-shaped sensor	0-250	$\|S_{21}\|$	6	500	0.0156 dB/(mg/dL)
34	T-shaped patterned MLIN	20-120 & 100-600	$\|S_{11}\|$	7.8 & 6	500	$1.2x10^{-2}$ & $5.4x10^{-3}$ dB/(mg/dL)
35	Monopole Antenna-Sensor	0-190	F_r (S_{11})	2.4	2	350 kHz/(mg/dL)
36	MC-CSRR	70-150	$\|S_{11}\|$ & $\|S_{21}\|$ & F_r (S_{11}) & F_r (S_{21})	1-6	400-1.200	$[5 - 21]x10^{-3}$ & $[3.3 - 9.8]x10^{-3}$ dB/(mg/dL) $[2.74 - 3.34]x10^{-1}$ & $[6.7 - 11]x10^{-2}$ kHz/(mg/dL)
38	Microstrip line (MLIN)	78-625 & 625-5.000	$\|S_{11}\|$	1.48	7.500	$6.6x10^{-3}$ & $1.8x10^{-3}$ dB/(mg/dL)
TW	Spurline sensor	0-150	$\|S_{11}\|$ & F_r (S_{11})	1.55-1.58	50	$7.82x10^{-3}$ dB/(mg/dL) & 233.33 kHz/(mg/dL)

NA-data not available, TW-this work

4. CONCLUSION

The proposed work presents a compact and simple microwave sensor for rapid detection of glucose concentration using a small volume, operating at low frequencies. The proposed work investigates and analyzes the relationships between glucose concentration levels, ranging from hypoglycemia to normoglycemia to hyperglycemia and the magnitudes of S_{11} and F_r. A mathematical model is developed to describe the correlation resulting from the response of the proposed sensor in each measured concentration range. The proposed sensor provides effective real-time detection, requires small samples, uses a simple methodology and operation, and is cost-effective for determining glucose concentration.

ACKNOWLEDGMENT

This research project was financially supported by the Mahasarakham University. We thank Prof. Dr. Prayoot Akkaraekthalin for the full-wave EM simulation program.

REFERENCES

[1] Majeed, A., El-Sayed, A. A., Khoja, T., Alshamsan, R., Millett, C., Rawaf, S. (2014). Diabetes in the Middle-East and North Africa: An update. *Diabetes Research and Clinical Practice*, 103 (2), 218-222. https://doi.org/10.1016/j.diabres.2013.11.008

[2] Segar, M. W., Patel, K. V., Vaduganathan, M., Caughey, M. C., Butler, J., Fonarow, G. C., Grodin, J. L., McGuire, D. K., Pandey, A. (2020). Association of long-term change and variability in glycemia with risk of incident heart failure among patients with type 2 diabetes: A secondary analysis of the ACCORD trial. *Diabetes Care*, 43 (8), 1920-1928. https://doi.org/10.2337/dc19-2541

[3] Shokrekhodaei, M., Quinones, S. (2020). Review of non-invasive glucose sensing techniques: Optical, electrical and breath acetone. *Sensors (Basel)*, 20 (5), 1251. https://doi.org/10.3390%2Fs20051251

[4] Uwadaira, Y., Ikehata, A., Momose, A., Miura, M. (2016). Identification of informative bands in the short-wavelength NIR region for non-invasive blood glucose measurement. *Biomedical Optics Express*, 7 (7), 2729-2737. https://doi.org/10.1364%2FBOE.7.002729

[5] Kino, S., Omori, S., Katagiri, T., Matsuura, Y. (2016). Hollow optical-fiber based infrared spectroscopy for measurement of blood glucose level by using multi-reflection prism. *Biomedical Optics Express*, 7 (2), 701-708. https://doi.org/10.1364%2FBOE.7.000701

[6] Sim, J. Y., Ahn, C. G., Jeong, E. J., Kim, B. K. (2018). In vivo microscopic photoacoustic spectroscopy for non-invasive glucose monitoring invulnerable to skin secretion products. *Scientific Reports*, 8 (1), 1059. https://doi.org/10.1038/s41598-018-19340-y

[7] Zheng, Y., Zhu, X., Wang, Z., Hou, Z., Gao, F., Nie, R., Cui, X., She, J., Peng, B. (2017). Noninvasive blood glucose detection using a miniature wearable raman spectroscopy system. *Chinese Optics Letters*, 15, 083001. https://opg.optica.org/col/viewmedia.cfm?uri=col-15-8-083001&seq=0

[8] Tiangco, C., Fon, D., Sardesai, N., Kostov, Y., Sevilla, F. III., Rao, G., Tolosa, L. (2017). Fiber optic biosensor for transdermal glucose based on the glucose binding protein. *Sensors and Actuators B: Chemical*, 242, 569-576. https://doi.org/10.1016/j.snb.2016.11.077

[9] Lan, Y. T., Kuang, Y. P., Zhou, L. P., Wu, G. Y., Gu, P. C., Wei, H. J., Chen, K. (2017). Noninvasive monitoring of blood glucose concentration in diabetic patients with optical coherence tomography. *Laser Physics Letters*, 14, 035603. http://dx.doi.org/10.1088/1612-202X/aa58c0

[10] Chen, H., Chen, X., Ma, S., Wu, X., Yang, W., Zhang, W., Li, X. (2018). Quantify glucose level in freshly diabetic's blood by terahertz time-domain spectroscopy. *Journal of Infrared, Millimeter, and Terahertz Waves*, 39, 399-408. https://doi.org/10.1007/s10762-017-0462-2

[11] Omer, A. E., Shaker, G., Safavi-Naeini, S., Kokabi, H., Alquié, G., Deshours, F., Shubair, R. M. (2020). Low-cost portable microwave sensor for non-invasive monitoring of blood glucose level: Novel design utilizing a four-cell CSRR hexagonal configuration. *Scientific Reports*, 10 (1), 15200. https://doi.org/10.1038/s41598-020-72114-3

[12] Martin, F., Velez, P., Munoz-Enano, J., Su, L. (2023). Introduction to planar microwave sensors. In *Planar Microwave Sensors*. Wiley-IEEE Press, 1-64. https://doi.org/10.1002/9781119811060.ch1

[13] Gonzales, W. V., Mobashsher, A. T., Abbosh, A. (2019). The progress of glucose monitoring-a review of invasive to minimally and non-invasive techniques, devices and sensors. *Sensors (Basel)*, 19 (4), 800. https://doi.org/10.3390/s19040800

[14] Turgul, V., Kale, I. (2017). Simulating the effects of skin thickness and fingerprints to highlight problems with mon-invasive RF blood glucose sensing from fingertips. *IEEE Sensors Journal*, 17, 7553-7560. https://doi.org/10.1109/JSEN.2017.2757083

[15] Hofmann, M., Fischer, G., Weigel, R., Kissinger, D. (2013). Microwave-based noninvasive concentration measurements for biomedical applications. *IEEE Transactions on Microwave Theory and Techniques*, 61, 2195-2204. https://doi.org/10.1109/TMTT.2013.2250516

[16] Yilmaz, T., Foster, R., Hao, Y. (2019). Radio-frequency and microwave techniques for non-invasive measurement of blood glucose levels. *Diagnostics*, 9 (1), 6. https://doi.org/10.3390/diagnostics9010006

[17] Saha, S., Cano-Garcia, H., Sotiriou, I., Lipscombe, O., Gouzouasis, I., Koutsoupidou, M., Palikaras, G., Mackenzie, R., Reeve, T., Kosmas, P., Kallos, E. (2017). A glucose sensing system based on transmission measurements at millimetre waves using micro strip patch antennas. *Scientific Reports*, 7 (1), 6855. https://doi.org/10.1038/s41598-017-06926-1

[18] Saeedi, S., Chammani, S., Fischer, G. (2022). Feasibility study of glucose concentration measurement of aqueous solution using time domain reflected signals. *Sensors (Basel)*, 22 (3), 1174. https://doi.org/10.3390/s22031174

[19] Mohamed, A. Z., Amar, R., Cherif, H., Hichem, A. (2021). Hyper-sensitive microwave sensor based on split ring resonator (SRR) for glucose measurement in water. *Sensors and Actuators A: Physical*, 321, 112601. https://doi.org/10.1016/j.sna.2021.112601

[20] Saeed, K., Shafique, M. F., Byrne, M. B., Hunter, I. C. (2012). Planar microwave sensors for complex permittivity characterization of materials and their applications. In *Applied Measurement Systems*. IntechOpen, 319-350. https://doi.org/10.5772/36302

[21] Alahnomi, R. A., Zakaria, Z., Yussof, Z. M., Althuwayb, A. A., Alhegazi, A., Alsariera, H., Rahman, N. A. (2021). Review of recent microwave planar resonator-based sensors: Techniques of complex permittivity extraction, applications, open challenges and future research directions. *Sensors (Basel)*, 21 (7), 2267. https://doi.org/10.3390/s21072267

[22] Morales-Lovera, H. N., Olvera-Cervantes, J. L., Perez-Ramos, A. E., Corona-Chavez, A., Saavedra, C. E. (2022). Microstrip sensor and methodology for the determination of complex anisotropic permittivity using perturbation techniques. *Scientific Reports*, 12 (1), 2205. https://doi.org/10.1038/s41598-022-06259-8

[23] Jang, C., Park, J. K., Lee, H. J., Yun, G. H., Yook, J. G. (2020). Non-invasive fluidic glucose detection based on dual microwave complementary split ring resonators with a switching circuit for environmental effect elimination. *IEEE Sensors Journal*, 20, 8520-8527. https://doi.org/10.1109/JSEN.2020.2984779

[24] Kumar, A., Wang, C., Meng, F. Y., Zhou, Z. L., Zhao, M., Yan, G. F., Kim, E. S., Kim, N. Y. (2020). High-sensitivity, quantified, linear and mediator-free resonator-based microwave biosensor for glucose detection. *Sensors (Basel)*, 20 (14), 4024. https://doi.org/10.3390/s20144024

[25] Satish, S. K., Anand, S. (2021). Demonstration of microstrip sensor for the feasibility study of non-invasive blood-glucose sensing. *Mapan - Journal of Metrology Society of India*, 6 (1), 193-199. https://doi.org/10.1007/s12647-020-00396-z

[26] Juan, C. G., Bronchalo, E., Potelon, B., Quendo, C., Muñoz, V. F., Ferrández-Vicente, J. M., Sabater-Navarro, J. M. (2023). On the selectivity of planar microwave glucose sensors with multicomponent solutions. *Electronics*, 12 (1), 191. https://doi.org/10.3390/electronics12010191

[27] Nakamura, M., Tajima, T., Seyama, M. (2022). Broadband dielectric spectroscopy for quantitative analysis of glucose and albumin in multicomponent aqueous solution. *IEEE Journal of Electromagnetics, RF and Microwaves in Medicine and Biology*, 6 (1), 86-93. https://doi.org/10.1109/JERM.2021.3096150

[28] Bakam Nguenouho, O. S., Chevalier, A., Potelon, J., Benedicto, J., Quendo, C. (2022). Dielectric characterization and modelling of aqueous solutions involving sodium chloride and sucrose and application to the design of a bi-parameter RF-sensor. *Scientific Reports*, 12, 7209. https://doi.org/10.1038/s41598-022-11355-w

[29] Juan, C. G., Potelon, B., Quendo, C., García-Martínez, H., Ávila-Navarro, E., Bronchalo, E., Sabater-Navarro, J. M. (2021). Study of Q_u-based resonant microwave sensors and design of 3-D-printed devices dedicated to glucose monitoring. *IEEE Transactions on Instrumentation and Measurement*, 70, 1-16. https://doi.org/10.1109/TIM.2021.3122525

[30] Govind, G., Akhtar, M. J. (2020). Design of an ELC resonator-based reusable RF microfluidic sensor for blood glucose estimation. *Scientific Reports*, 10, 18842. https://doi.org/10.1038/s41598-020-75716-z

[31] Juan, C. G., Potelon, B., Quendo, C., Bronchalo, E. (2021). Microwave planar resonant solutions for glucose concentration sensing: A systematic review. *Applied Sciences*, 11, 7018. https://doi.org/10.3390/app11157018

[32] Turgul, V., Kale, I. (2018). Permittivity extraction of glucose solutions through artificial neural networks and non-invasive microwave glucose sensing. *Sensors and Actuators A: Physical*, 277, 65-72. https://doi.org/10.1016/j.sna.2018.03.041

[33] Odabashyan, L., Babajanyan, A., Baghdasaryan, Z., Kim, S., Kim, J., Friedman, B., Lee, J. H., Lee, K. (2019). Real-time noninvasive measurement of glucose concentration using a modified hilbert shaped microwave sensor. *Sensors (Basel)*, 19 (24), 5525. https://doi.org/10.3390/s19245525

[34] Omkar, Yu, W., Huang, S. Y. (2018). T-shaped patterned microstrip line for moninvasive continuous glucose sensing. *IEEE Microwave and Wireless Components Letters*, 28 (10), 942-944. https://doi.org/10.1109/LMWC.2018.2861565

[35] Gharbi, M. E., Fernández-García, R., Gil, I. (2021). Textile antenna-sensor for in vitro diagnostics of diabetes. *Electronics*, 10, 1570. https://doi.org/10.3390/electronics10131570

[36] Omer, A. E., Shaker, G., Safavi-Naeini, S., Ngo, K., Shubair, R. M., Alquie, G., Deshours, F., Kokabi, H. (2021). Multiple-cell microfluidic dielectric resonator for liquid sensing applications. *IEEE Sensors Journal*, 5, 6094-6104. https://doi.org/10.1109/JSEN.2020.3041700

[37] Hanna, J., Tawk, Y., Azar, S., Ramadan, A. H., Dia, B., Shamieh, E., Zoghbi, S., Kanj, R., Costantine, J., Eid, A. A. (2022). Wearable flexible body matched electromagnetic sensors for personalized non-invasive glucose monitoring. *Scientific Reports*, 12 (1), 14885. https://doi.org/10.1038/s41598-022-19251-z

[38] Huang, S. Y., Omkar, Yoshida, Y., Garcia Inda, A. J., Xavier, C. X., Mu, W. C., Meng, Y. S. (2019). Microstrip line-based glucose sensor for noninvasive continuous monitoring using the main field for sensing and multivariable crosschecking. *IEEE Sensors Journal*, 19 (2), 535-547. https://doi.org/10.1109/JSEN.2018.2877691

[39] Zidane, M. A., Rouane, A., Hamouda, C., Amar, H. (2021). Hyper-sensitive microwave sensor based on split ring resonator (SRR) for glucose measurement in water. *Sensors and Actuator A: Physical*, 321, 112601. https://doi.org/10.1016/j.sna.2021.112601

[40] Baghelani, M., Abbasi, Z., Daneshmand, M., Light, P. E. (2020). Non-invasive continuous-time glucose monitoring system using a chipless printable sensor based on split ring microwave resonators. *Scientific Reports*, 10 (1), 12980. https://doi.org/10.1038/s41598-020-69547-1

[41] Mohammadi, S., Wiltshire, B., Jain, M. C., Nadaraja, A.V., Clements, A., Golovin, K., Roberts, D.J., Johnson, T., Foulds, I., Zarifi, M.H., (2020). Gold coplanar waveguide resonator integrated with a microfluidic channel for aqueous dielectric detection. *IEEE Sensors Journal*, 20 (17), 9825-9833. https://doi.org/10.1109/JSEN.2020.2991349

Received March 22, 2023
Accepted July 31, 2023